

Magnetic Elastic Scattering of Electrons by Light Nuclei*

J. GOLDEMBERG† AND Y. TORIZUKA‡

High-Energy Physics Laboratory, Stanford University, Stanford, California

(Received 6 August 1962)

The elastic scattering of 41.5-MeV electrons was measured at $\sim 180^\circ$ where the charge scattering is very small so magnetic scattering stands out more clearly. Measurements were made for ${}^1\text{H}^1$, ${}^1\text{D}^2$, ${}^2\text{He}^4$, ${}^3\text{Li}^6$, ${}^3\text{Li}^7$, ${}^4\text{Be}^9$, ${}^6\text{Be}^{10}$, ${}^6\text{B}^{11}$, ${}^6\text{C}^{12}$, ${}^7\text{N}^{14}$, ${}^8\text{O}^{16}$, ${}^9\text{F}^{19}$, ${}^{10}\text{Ne}^{20}$, ${}^{11}\text{Na}^{23}$, ${}^{12}\text{Mg}$, ${}^{13}\text{Al}^{27}$, ${}^{15}\text{P}^{31}$, ${}^{18}\text{Ar}^{40}$, ${}^{19}\text{K}^{39}$, and ${}^{20}\text{Ca}^{40}$. It is shown that the results are consistent with calculations based on scattering by the magnetic moment of the nuclei involved.

I. INTRODUCTION

THE magnetic elastic scattering of high-energy electrons in the proton and deuteron has been intensively investigated by Hofstadter and collaborators¹ and some of their important properties established.

It is clear that other nonzero spin nuclei will exhibit magnetic elastic scattering under conditions in which the charge scattering is not completely dominant.

The relative order of magnitude of the magnetic moment effects in scattering can be established very simply.² The measure of the strength of the Coulomb interaction is Ze (Z atomic number, e electronic charge); the measure of the magnetic moment interaction is $q\mu$, where q is the momentum transfer and μ the magnetic moment of the nucleus.

The relative size of the two effects will therefore be of the order of magnitude

$$\frac{q\mu}{eZ} = \frac{1}{2Mc} \frac{q}{Z} \frac{\mu}{\mu_N}, \quad (1)$$

where M is the nucleon mass and μ_N the nuclear magneton.

It is seen that the relative effects of magnetic scattering will be largest for small Z and for nuclei with large magnetic moments.

We will report in this paper measurements of the elastic scattering of 41.5 MeV at $\sim 180^\circ$ where the charge scattering is very small and so the magnetic contribution can be more clearly seen. Our investigation covered most of the light elements up to ${}^{20}\text{Ca}^{40}$.

Our energy was not high enough to evidence the effects of the form factors for magnetic scattering, which are expected to fall off more rapidly with increasing q than the charge scattering form factors since the magnetic effects reside in the surface according to the shell model.

II. EXPERIMENTAL ARRANGEMENT AND PROCEDURE

The experimental arrangement for 180° scattering in use in the Mark II Linac at Stanford University was described previously.³ Figure 1 shows only a sketch of the apparatus. Electrons from the incident beam are deflected $\sim 10^\circ$ before striking the target and the ones that undergo 180° scattering are deflected again by another 10° in the same auxiliary magnet before entering a magnetic spectrometer located at 160° with respect to the incident beam.

Some of the targets used were gases and a special gas target was constructed to contain them; it was a cylinder 3-in. diameter and 12 in. long with a 5-mil dural entrance window. A previous experiment showed that the efficiency of detection of scattering particles decreased rapidly as the target was moved away from the entrance window; the effective thickness of the gas target was determined by comparison with a solid target.

The solid targets were in the form of disks about $1\frac{1}{2}$ in. in diameter and thicknesses that were of the order of $\frac{1}{16}$ in. Table I lists all the targets used with relevant information.

It was found that multiple scattering in the thicker solid targets could be appreciable; the reason is that the spectrometer has a finite angle of entrance which is ~ 0.0038 sr; since the Mott cross section is zero at 180° but increases very rapidly for smaller angles, multiple scattering tends to throw in the spectrometer electrons scattered at smaller angles. Our thickest targets were 0.01 radiation length thick (see Table I) but this corresponds to an average scattering angle large enough to have an effect in the experiment.

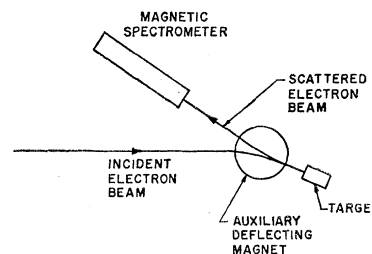


FIG. 1. Sketch of experimental arrangement for 180° scattering (not to scale).

* This work was supported in part by the joint program of the Office of Naval Research, the U. S. Atomic Energy Commission, and Air Force Office of Scientific Research.

† On leave from University of São Paulo, São Paulo, Brazil.

‡ On leave from Tohoku University, Sendai, Japan.

¹ R. Hofstadter, *Ann. Rev. Nucl. Sci.* **7**, 231 (1957).

² R. G. Newton, *Phys. Rev.* **103**, 385 (1956).

³ G. Peterson and W. C. Barber, *Phys. Rev.* **128**, 812 (1962).

TABLE I. Magnetic elastic cross sections.

Element	Spin	μ Magnetic moment (nm)	Target	Thickness (mg/cm ²)	Thickness (radiation lengths)	Experimental ^a elastic cross section (10 ⁻³² cm ² /sr)	Theoretical magnetic elastic cross section (10 ⁻³² cm ² /sr)
¹ H ¹	1/2	2.79	CH ₂	233	0.0052	7.5 ± 0.3	9.40
...	Gas	33.5	0.00058
¹ D ²	1	0.857	Gas	28.8	0.00050	0.55 ± 0.06	0.59
² He ⁴	0	0	Gas	29.0	0.00034	0.02 ± 0.3	0
³ Li ⁶	1	0.82	Metal	149	0.0028	0.8 ± 0.4	0.54
³ Li ⁷	3/2	3.26	Metal	170	0.0028	5.6 ± 0.5	7.10
⁴ Be ⁹	3/2	1.18	Metal	146	0.0025	1.1 ± 0.5	0.93
⁵ B ¹⁰	3	1.80	Metal	148	0.0030	5.3 ± 0.6	1.72
⁵ B ¹¹	3/2	2.69	Metal	203	0.0040	5.5 ± 0.6	4.90
⁶ C ¹²	0	0	Graphite	125	0.0028	0.2 ± 0.6	0
⁷ N ¹⁴	1	0.40	Gas	200	0.0050	0.7 ± 0.7	0.125
⁸ O ¹⁶	0	0	Gas	228	0.0065	0 ± 1.0	0
⁹ F ¹⁹	1/2	2.63	CF ₂	150	0.0061	2.8 ± 2.6	8.30
¹⁰ Ne ²⁰	0	0	Gas	143	0.0050	0 ± 1.5	0
¹¹ Na ²³	3/2	2.22	Metal	150	0.0054	4.0 ± 2.5	3.25
¹² Mg	0	0	Metal	174	0.0068	0 ± 2.5	0
¹³ Al ²⁷	5/2	3.64	Metal	101	0.0040	4.4 ± 3.3	7.50
¹⁵ P ³¹	1/2	1.13	Red phosphorus	241	0.011	4.0 ± 4.0	1.52
¹⁸ Ar ⁴⁰	0	0	Gas	205	0.014	-1.0 ± 4.0	0
¹⁹ K ³⁹	3/2	0.39	Metal	135	0.0074	1.0 ± 4.0	-0.09
²⁰ Ca ⁴⁰	0	0	Metal	98	0.0054	-1.0 ± 6.7	0

^a The charge scattering contribution to the cross section was subtracted.

Figure 2 shows typical elastic peaks measured for 3 different thicknesses of Al; the peaks are broader and shifted to lower energies for the heavier targets as a result of energy loss and straggling of the electrons.

Figure 3 shows the area under the elastic peaks of Fig. 2 measured down to 3% from the maximum as a function of thickness. It is seen that deviations from linearity occur although they are small for the targets used in this experiment. A correction was made whenever necessary. The acceptance angle for the gas targets was smaller than for the solid targets due to their effective thickness and a correction was also made for that.

These corrections are only important for the charge scattering which is so strongly dependent on angle at $\sim 180^\circ$; the magnetic scattering is much less dependent on angle.

In all experiments scattering in the windows was not negligible and target out runs were made so that this background could be subtracted.

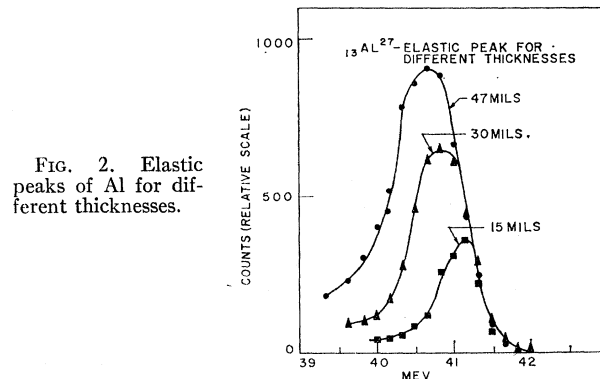


FIG. 2. Elastic peaks of Al for different thicknesses.

III. DATA

Elastic peaks were measured for the elements listed in Table I. Typical elastic peaks are shown in Fig. 4; the areas were measured down to 3% of elastic-peak maximum and compared to the proton peak obtained from a CH₂ target and from an H₂ gas target.

The proton cross section is well known from the work of Hofstadter *et al.*⁴:

$$\frac{d\sigma}{d\Omega} = \left(\frac{e^2}{2E_0} \right)^2 \frac{\cos^2(\theta/2)}{\sin^4(\theta/2)} \frac{1}{1 + (2E_0/Mc^2) \sin^2(\theta/2)} \times \left\{ F_1^2 + \frac{\hbar^2 q^2}{4M^2 c^2} [2(F_1 + kF_2)^2 \tan^2(\theta/2) + k^2 F_2^2] \right\}, \quad (2)$$

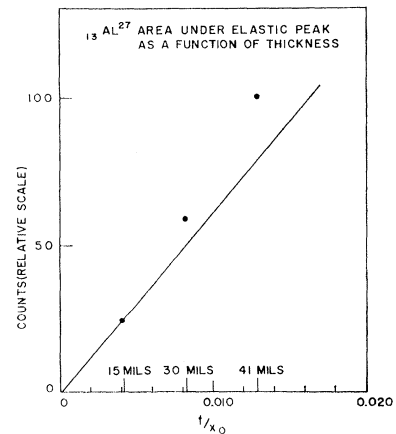


FIG. 3. Elastic peak area as a function of thickness from the curves of Fig. 2; t/x_0 is the thickness in radiation lengths.

⁴ R. Hofstadter, F. Bumiller, and M. R. Yearian, *Revs. Mod. Phys.* **30**, 482 (1958).

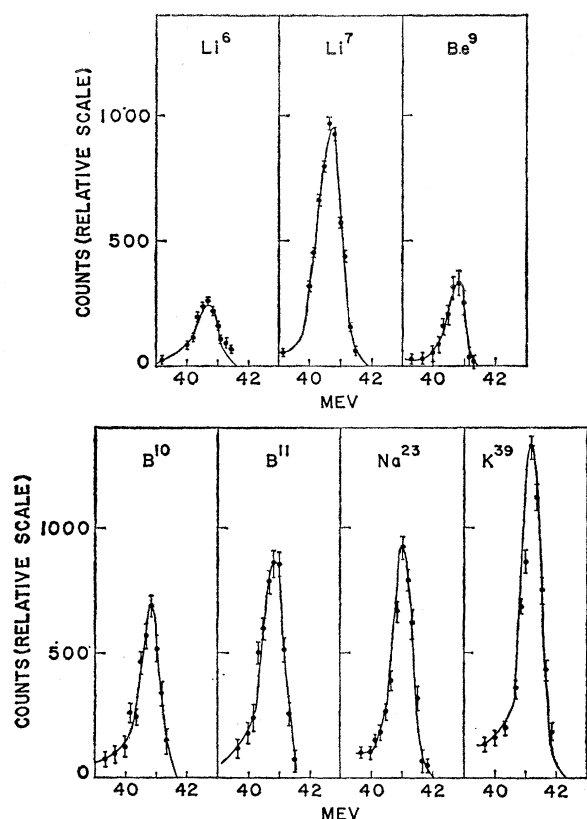


FIG. 4. Typical elastic-peak curves.

where

$$q = \frac{(2E_0/\hbar c) \sin(\theta/2)}{[1 + (2E_0/Mc^2) \sin^2(\theta/2)]^{1/2}}, \quad (3)$$

$F_1=0.985$ (proton's Dirac form factor), $F_2=0.980$ (proton's Pauli form factor), $k=1.7926$, and M =proton mass. All of our cross sections were normalized to the

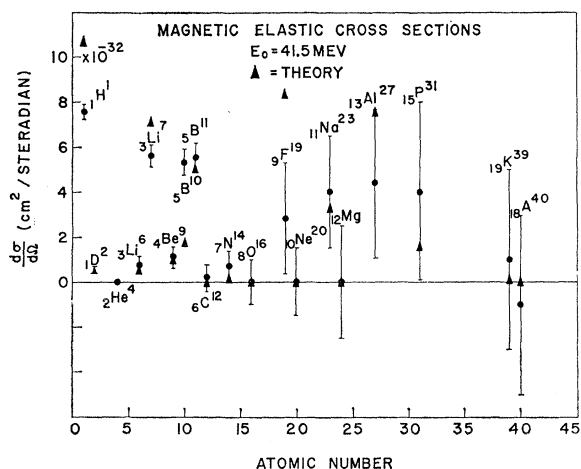


FIG. 5. Elastic magnetic cross sections at $\sim 180^\circ$. The theoretical points are obtained from formula (4) in the text which does not take recoil into account.

value given by formula (2) at $E_0=41.5$ MeV. The results are listed in Table I.

For the heavier elements the Mott scattering becomes very important; since the magnetic scattering is due always to one or a few unpaired nuclei it does not change much as Z increases and the magnetic scattering becomes a smaller fraction of the total; consequently the errors for the heavier nuclei become much larger.

DISCUSSION

In Fig. 5 we subtracted the charge scattering contribution to our data and have thus left the magnetic scattering cross section. The theoretical points were obtained from the following expression which gives the magnetic scattering cross section from a point nucleus of charge Z and magnetic moment K .^{5,6}

$$\frac{d\sigma}{d\Omega} = \sigma_{\text{charge}} + \sigma_{\text{magnetic}} \\ = \sigma_{\text{Mott}} \left\{ F_c^2 + \frac{J+1}{3J} \frac{K^2}{Z^2} \frac{\hbar^2 q^2}{4M^2 c^2} [1 + 2 \tan^2(\frac{1}{2}\theta)] \right\}, \quad (4)$$

$$\sigma_{\text{Mott}} = \left(\frac{Ze^2}{2E_0} \right)^2 \frac{\cos^2(\frac{1}{2}\theta)}{\sin^4(\frac{1}{2}\theta)}, \quad (5)$$

where $q = (2E_0/\hbar c) \sin(\theta/2)$, J =spin of nucleus, M =nucleon mass, K is the static magnetic moment in nuclear magnetons, $K = [\mu/(e\hbar/Mc)]$ (μ =magnetic moment), and F_c =charge scattering form factor.

This formula is valid if one neglects recoil and considers only the $M1$ matrix element which is dominant for low momentum transfers.⁷ In the backward direction ($\theta \rightarrow \pi$) it is a generalization of the Rosenbluth formula for a point nucleus with any J and a magnetic moment μ .

There are two ways in which the scattering can differ from that given by the static magnetic moment.

(i) The magnetic moment can have a structure and hence a form factor must enter in formula (4) which in general will decrease the cross section for scattering.

(ii) The cross section will always increase due to contribution of higher multipoles since the selection rules for magnetic elastic scattering are:

$$1 \leq L \leq 2J, \\ \text{no parity change.}$$

⁵ J. Scofield (private communication).

⁶ J. M. Jauch, *Helv. Phys. Acta* **13**, 541 (1940); see also R. Gatto, *Nuovo Cimento* **12**, 613 (1954).

⁷ Note added in proof. Phase shift calculations of the charge scattering at $\sim 180^\circ$ were made recently by R. Herman and D. G. Ravenhall (private communication), and for the momentum transfers and atomic numbers involved here, small errors are committed if one uses for the charge scattering the values given by the Born approximation.

These two effects tend to compensate each other in cases where the spin of the bombarded nucleus is large.

A complete expression for magnetic scattering by finite-size nuclei with a magnetic momentum was derived by Walecka and Pratt⁸; the connection with Rosenbluth's formula is discussed there.

From Fig. 5 it is seen that for light elements, where magnetic scattering is big and thus our error (due to subtracting the charge cross section) is small, the experimental points follow the theory quite closely. ${}^6\text{B}^{10}$ seems to be the only exception. Since it has a large spin, this might be due to contributions of higher multipoles which are not present in ${}^6\text{B}^{11}$. For heavier nuclei the errors are large, and there seem to be no major conflicts between theory and experiment. The H theoretical point is higher than the experimental because no recoil is assumed in formula (4) which makes an appreciable effect only in H, and removes completely the discrepancy when taken into account.

For the case of Li^7 a calculation of the scattering cross section was made by Willey,⁹ using known wave functions for the ground state of Li^7 . The calculations were made for a *LS* coupling and for an odd-proton model.

⁸ J. D. Walecka and R. H. Pratt (private communication).

⁹ R. Willey (private communication).

The results are listed below for 41.5 MeV:

<i>LS</i> model,	3.70×10^{-32} cm ² /sr;
Odd-proton model,	5.71×10^{-32} cm ² /sr;
Formula (4),	7.1×10^{-32} cm ² /sr;
Experiment,	5.6×10^{-32} cm ² /sr.

Although the magnetic moment in Li^7 is in agreement with the predictions of the *LS* model, the old proton model is considerably better than the *LS* model in predicting the scattering results.

The case of He^4 is very special because the absence of magnetic scattering can yield information on an electric dipole moment of the electron. It will be discussed in another publication.¹⁰

Further work on the lighter nuclei with higher electron energies would be very interesting because of the expected sharp decrease in cross section due to the effect of the magnetic form factors.

We wish to thank Dr. W. C. Barber for constant encouragement and advice, Dr. G. A. Peterson who participated in the initial phases of the work, Prof. R. Hofstadter, Dr. J. Scofield, Dr. J. D. Walecka, and Dr. R. H. Pratt for stimulating discussions, and J. Carson and E. Wright for generous technical help. One of us (Y. T.) wishes to thank the Ministry of Education of Japan which made possible his stay at Stanford.

¹⁰ J. Goldemberg and Y. Torizuka (to be published).

Beta-Gamma Directional Correlation in Re^{188} †

L. D. WYLY, C. H. BRADEN, AND HARRY DULANEY

School of Physics, Georgia Institute of Technology, Atlanta, Georgia

(Received 11 June 1962; revised manuscript received 19 September 1962)

The directional correlation between the 1960-keV beta group and the 155-keV gamma in the decay of Re^{188} has been measured. The coefficient A_2 is found to vary from about 0.17 to about 0.25 over the energy range $W=3$ to $W=4.3$. Limitations on the matrix elements for the sequence $1^-(\beta)2^+(\gamma)0^+$ are discussed. It is found that the directional correlation and a variety of beta spectral shapes may be fitted for values of the parameter $|\zeta_1|$ greater than some minimum value which is dependent upon the spectral shape. Information is presented on further limitations of the matrix elements which will result when the shape is known and some discussion is given for the role of a measurement of the beta-circularly polarized gamma correlation.

EXPERIMENTAL PROCEDURE AND RESULTS

THE 17-h Re^{188} was purchased from the Oak Ridge National Laboratory as processed, high specific activity (~ 20 mC/ml) 91-h Re^{186} . At the time of assay before leaving Oak Ridge the Re^{188} activity was approximately one-third of the total activity. Sources were prepared by evaporation of the nitric acid solution of the HReO_4 on 0.25-mil Mylar backing. The sources were transparent. They were grounded by a thin

Aquadag line. Data taking for the directional correlation determination began about eight hours subsequent to the assay at Oak Ridge.

The electronic equipment and general experimental procedure has been previously described.¹ The decay scheme of Re^{188} is shown in Fig. 1.² A single-channel

¹ Harry Dulaney, C. H. Braden, E. T. Patronis, Jr., and L. D. Wyly, *Phys. Rev.* **129**, 283 (1963).

² *Nuclear Data Sheets*, Natl. Acad. Sci.-Natl. Res. Council, NRC 59-3-119 (Office of Printing and Publishing, National Research Council-National Academy of Sciences, Washington 25, D. C.).

† Supported in part by a grant from the National Science Foundation (G6337).